Evaluating the possible role of ^{68}Ga-citrate PET/CT in the characterization of indeterminate lung lesions

Mariza Vorster · Alex Maes · Aldrich Jacobs · Sidney Malefahlo · Hans Pottel · Christophe Van de Wiele · Machaba Mike Sathekge*

Abstract We sought to determine whether PET/CT imaging with ^{68}Ga-citrate could be of value in distinguishing benign from malignant lung pathology in a setting with a high prevalence of granulomatous diseases.

Methods Thirty-six consecutive patients with indeterminate lung lesions prospectively underwent dual time point (60 and 120 min) ^{68}Ga-citrate PET/CT study prior to lung biopsy. Qualitative and semi-quantitative measures of tracer uptake in the lung lesions (SUVmax) were compared to the histopathology in order to establish an imaging pattern to distinguish benign from malignant lesions.

Results Fourteen patients (38.9 %) were diagnosed with a malignant lesion, 12 (33.3 %) with tuberculosis (TB), and 10 participants (27.8 %) with other benign lung lesions. At 60-min post-injection, patients who were diagnosed with a malignant lesion ($n = 14$) demonstrated a mean SUVmax of 3.36 ± 1.14, with a median value of 3.04 (min = 1.56, max = 4.65).Those with TB ($n = 12$) demonstrated a SUVmax of 3.99 ± 2.28, and a median value of 3.71 ($pct_{25} = 2.19$, $pct_{75} = 4.95$). In patients with other benign lesions ($n = 10$), the following values were observed: a SUVmax of 2.70 ± 1.31, a median value of 2.50 ($pct_{25} = 1.76$, $pct_{75} = 3.59$). The mean values of these three types of pathology were not statistically significant ($p = 0.1919$), and therefore the SUVmax could not be used to accurately distinguish between these lesions using both early and delayed imaging.

Conclusion This study, as the first ^{68}Ga-citrate PET/CT in humans for the in vivo imaging of lung pathology, demonstrated its potential for the detection of both malignancy and TB. However, ^{68}Ga-citrate seemed incapable of providing a clear distinction between malignant and benign lung lesions in a setting with a high prevalence of granulomatous diseases such as TB.

Keywords ^{68}Ga-citrate · PET · Lung lesions

M. Vorster · M. M. Sathekge *
Department of Nuclear Medicine, University of Pretoria and Steve Biko Academic Hospital,
Private Bag X169, Pretoria 0001, South Africa
e-mail: mike.sathekge@up.ac.za; sathekgemike@gmail.com

M. Vorster
e-mail: marizavorster@gmail.com

A. Maes · H. Pottel
Department of Nuclear Medicine, AZ Groeninge,
Reepkaai, Kortrijk, Belgium
e-mail: alex.maes@azgroeninge.be

H. Pottel
e-mail: Hans.Pottel@kuleuven-kortrijk.be

A. Jacobs · S. Malefahlo
Department of Cardiothoracic Surgery, University of Pretoria and Steve Biko Academic Hospital, Pretoria, South Africa
e-mail: aldrich.jacobs@up.ac.za

S. Malefahlo
e-mail: Sidney.malefahlo@up.ac.za

C. Van de Wiele
Department of Nuclear Medicine, University Hospital Ghent,
Ghent, Belgium
e-mail: christophe.vandewiele@UGent.be

Introduction

PET/CT imaging plays an important role in the characterization of solitary pulmonary nodules (SPN) and has been one of the first indications for which medical schemes have agreed to reimburse. However, in the South African setting, SPN and other lung lesions of an indeterminate nature, continue to present physicians with a diagnostic

challenge. This is mainly due to the high prevalence of granulomatous diseases such as tuberculosis (TB), which is frequently associated with human immunodeficiency virus (HIV).

Various studies have indicated the inability of ^{18}F-FDG-PET/CT, despite the use of dual phase imaging, to distinguish accurately between benign and malignant causes of SPN in the setting of a high TB prevalence [1–3]. This is due to the similar behavior over time of malignant and granulomatous lesions in terms of FDG uptake and this has also been confirmed in our setting [4–6]. Multiple tests are often required which still often ultimately require biopsy for histological confirmation [7].

An increase in the availability and accessibility of PET/CT facilities has sparked renewed interest in generator-based PET radiopharmaceuticals. Gallium-68, in particular, has received attention as an alternative positron emitter since it is not limited by the need for a nearby cyclotron and may be especially valuable in the imaging of infection/inflammation. Gallium (in the form of ^{67}Ga-citrate) has long provided nuclear physicians with a versatile tool for use in both oncological and infective settings [8, 9].

The mechanism of action, although incompletely explained, is generally accepted to be the result of various specific and non-specific factors, which play a role in both malignant and infective/inflammatory processes. Non-specific factors include the increased vascular permeability found in areas of inflammation or increased vascularity, whereas specific factors comprise both transferrin-dependent and transferrin-independent mechanisms. Gallium acts as an iron analog, the majority of which is bound to transferrin in plasma and then internalized as a gallium–transferrin complex into cells with expression of transferrin receptors. Other localization mechanisms include binding to lactoferrin, siderophores and leukocytes [8, 10, 11].

It therefore stands to reason that Ga-68 would be as useful as Ga-67 with the added advantages of improved image resolution, quantification possibilities, improved dosimetry and imaging logistics gained from PET/CT technology. Compared to ^{18}F-FDG, ^{68}Ga offers shorter imaging times and on-demand, year-round tracer availability that negates the need for an onsite or nearby cyclotron. This could have significant financial implications, which may lead to a more cost-effective way of imaging. In addition, the short half-life of 68 min provides attractive peptide labeling options for novel diagnostic and therapeutic applications [12].

Several authors have investigated the use of ^{68}Ga-citrate in the evaluation of various infectious and inflammatory conditions. So far, the most promising results have been found with the imaging of musculoskeletal infections [13, 14].

The aim of the present study was to evaluate the diagnostic accuracy of ^{68}Ga-citrate in distinguishing benign from malignant lesions in the lung.

Materials and methods

Approval was granted by the University of Pretoria's research ethics committee (No. 93/2011) and informed consent was obtained from all study participants prior to injection and imaging. Patients were recruited prospectively from the referring departments and imaged consecutively at the department of Nuclear Medicine, Steve Biko Academic Hospital, Pretoria, South Africa.

Patient population

Patients with lung pathology of an uncertain nature (e.g. lung mass, nodules/infiltrates detected on morphological imaging) and who were being considered for lung biopsy were included in this study, while patients with lung lesions that had remained stable for >2 years were excluded.

^{68}Ga-citrate preparation and QC

A SnO_2-based ^{68}Ge/^{68}Ga generator (iThemba LABS, Somerset West, South Africa) [15] was fractionally eluted with 10 ml of 0.6 N HCl for ^{68}Ga-citrate synthesis. This was performed manually in a one-step-aseptic procedure, which was based on a combination of the protocols used by Kumar et al. [16] and Rizzello et al. [17] and made use of ACD-A. All solvents used were of a pharmacological grade. For labeling with ^{68}Ga, anticoagulant citrate dextrose solution, USP formula A (ACD-A) was purchased as sterile and non-pyrogenic solution from Fenwal Inc. (Lake Zurich, IL, USA). The aqueous solution of ACD-A contains 2.20 % sodium citrate dehydrate, 0.73 % citric acid anhydrous and 2.45 % glucose monohydrate. A 30 % solution of supra-pure grade hydrochloric acid (HCl) was purchased from Merck Sharp & Dohme (Readington, NJ, USA). Quality control was performed prior to injection with both ITLC- and pH strips.

PET/CT imaging protocol

Study participants were imaged on a Siemens Biograph 40 PET/CT scanner 60 and 120 min post IV ^{68}Ga-citrate administration. Both oral (Barium in water) and IV contrast (100 ml Ultravist, at a rate of 2 ml/s) were administered, except where a contra-indication, such as inadequate kidney function or an allergy to iodine existed. Images were acquired in a three-dimensional mode with a 4-min emission scan for each of, on average, 7–9 bed positions (matrix

size 512 × 512) from the skull base to the pelvis. Reconstruction of images with and without attenuation correction (CT based) were done using OSEM (ordered subset expectation maximization) to yield axial, sagittal and coronal slices. For diagnostic CT, the following parameters were used: collimation of 24 × 1.2 mm, gantry rotation time of 500 ms, tube voltage of 120 kV, effective tube current of 100 mAs with online tube current modulation, and table feed of 18 mm/rotation. Contrast enhancement was achieved by intravenous administration of 100 ml of nonionic contrast material (Ultravist; Bayer HealthCare Pharmaceuticals) at a rate of 2 ml/s. The matrix size was 512 × 512. CT contrast-enhanced images were analyzed for characterization of the lung lesions by 2 experienced radiologists who were unaware of the clinical diagnosis or ^{68}Ga-citrate PET findings.

Image analysis

Images were analyzed by two experienced nuclear physicians and two radiologists independently. All images were first evaluated qualitatively for abnormal uptake, which if present, was then followed by semi-quantification analysis. We made use of the following scale with the liver intensity[1] as reference point in order to grade Gallium uptake:

1. 0 = no uptake.
2. 1 = uptake less intense than the liver.
3. 2 = uptake equal in intensity to the liver.
4. 3 = uptake more intense than the liver.

Semi-quantitative analysis was done as follows: a region of interest was manually drawn around any lung lesion and the size selected to correspond to the pathology on CT. This results in a standard uptake value (SUV), which is representative of the relative concentration of radiotracer in a lesion of interest, normalized to the patient's weight and the dose of radiotracer administered (SUV = radiotracer activity × patient weight/injected dose). We used the maximum SUV (SUVmax) in this study, which represents the voxel with the highest tracer uptake in the lesion. The SUVmax was recorded and compared to the SUVmax of various reference points, such as the mediastinal blood pool, the liver, spleen and bone marrow in order to calculate various ratios. Where dual time point imaging was performed ($n = 20$), a second SUVmax was recorded. The 60-min value was labeled $SUVmax_1$ and the 120 min image $SUVmax_2$. The change in SUVmax was calculated using the difference between the two SUVmax values divided by the initial value (and expressed as a percentage change): difference between $SUVmax_1$ and $SUVmax_2$/$SUVmax_1 \times 100$.

Results validation

Image findings were validated by comparing the PET/CT results to that of biopsy, tracheal aspirates, sputum microscopy and cultures, biochemistry and results of other conventional imaging modalities (CXR, CT, MRI and ultrasound).

In order to compare the accuracy of PET to that of CT using histology as the gold standard, the following criteria for expected uptake of ^{68}Ga-citrate were set:

- Making use of the qualitative assessment or visual score, the following patterns of uptake were used to provide clinically useful distinctions between various types of lung pathologies:
  - Benign lesions: no or very little ^{68}Ga-citrate uptake (grade 0 or 1).
  - Malignant lesions: similar to or more intense than the liver (grade 2 or 3).

PET was therefore considered correct whenever these patterns were present. CT was characterized according to the established patterns [2, 4] and compared to histology.

Statistical methods

Descriptive statistics were used to report patient characteristics and procedural details. Summary statistics is presented as mean (SD, standard deviation) or as median (IQR, interquartile range) in case of non-normality of the data. Numbers or percentages are reported otherwise. Statistical analysis was performed with SAS version 9.3. Differences in the SUVmax (and various lesion to background ratios) between benign and malignant lung lesions were assessed using unpaired t test to find mean values that are significantly different from each other. Statistical significance was defined as $p < 0.05$.

Results

Procedural details

The average injected dose of ^{68}Ga-citrate was 196 MBq (155–255 MBq). The average radiochemical purity determined by ITLC-SG was 98.9 ± 0.94 % which was confirmed by HPLC. The pH value of the product for injection was 4.0–4.5. All other requirements for QC were met. Intravenous contrast was administered to 23 patients (omitted in patients with sub-optimal kidney functions,

[1] The liver was chosen as the reference point based on similar scales used with ^{67}Gallium-citrate in other studies [18]. Also, the liver did not demonstrate any statistically significant difference in SUVmax between patients with benign or malignant lesions ($p = 0.9292$).

iodine allergy or a recent contrasted CT) and all study participants received oral contrast. No serious side effects were reported. (Three patients reported a burning sensation upon injection, which resolved upon dilution with normal saline.)

Images were acquired at 60- and 120-min post-injection and the change in SUV was calculated. High-quality images were obtained at 60-min post-injection without the need for any patient preparation.

Patient population

Thirty-six consecutive patients with lung lesions of an indeterminate nature were prospectively recruited and imaged at the Department of Nuclear Medicine, at the Steve Biko Academic Hospital, Pretoria, South Africa. Study participants included 20 males and 16 females with a median age of 52.5 years. The demographics were as follows: Black (56 %), Caucasian (36 %) and a smaller group consisting of Asian and Coloured participants (8 %). Five of the 36 patients were confirmed to be HIV positive (14 %) and 47.2 % were smokers.

Patients most commonly presented with a lung lesion localized to the upper lobe of the right lung (39 %). Histological or tissue confirmation could be obtained in 27/36 (75 %) and the remaining 25 % of diagnoses were reached based on combination of clinical, biochemical and other imaging findings. The final diagnoses were distributed as follows: 14 patients (38.9 %) were diagnosed with a malignant lesion, 12 patients (33.34 %) with TB and the remaining 10 participants (27.8 %) were diagnosed with other benign lung lesions (fibrosis, infective or inflammatory lesions and sarcoidosis).

We found no difference in gender distribution between patients with benign ($n = 22$) and malignant lung lesions ($n = 14$) using Fischer's exact test ($p = 1$). There was, however, a statistically significant difference ($p = 0.0080$) in the mean age distribution between these two groups: patients with a benign lesion had a mean age of 47.2 (13.1) compared to 58.9 (10.7).

The proportion of smokers in the benign group (44 %) vs. those with a malignancy (75 %) was not statistically significant ($p = 0.1414$). The localization of the primary lung lesion was also not significantly different with the majority of lesions in both groups presenting in the right upper lobe ($p = 0.3011$).

Image analysis

Image acquisition performed at 60-min post-injection of (on average) 185 MBq of ^{68}Ga-citrate resulted in good quality images. The quality of the images deteriorated significantly at 120 min, causing the target to background ratio to become unfavorable for interpretation.

Fig. 1 ^{68}Ga-citrate bio-distribution

The normal bio-distribution of ^{68}Ga-citrate is represented in Fig. 1 [14, 17].

Typical SUV (max) in the areas of normal ^{68}Ga-citrate bio-distribution was as follows: bone marrow: 4.0 (3.0–4.4), liver: 4.8 (3.84–5.8), mediastinal blood pool: 5.6 (4.3–7.2), spleen: 3.4 (2.9–4.2). These values were obtained by adding the SUVmax for the particular organ of every patient and calculating the median value. Values in brackets represent the 25th percentile to the 75th percentile.

SUVmax at 60 min post-injection

Patients who were diagnosed with a malignant lesion ($n = 14$) demonstrated a mean SUVmax of 3.36 ± 1.14, with a median value of 3.04 (min = 1.56, max = 4.65).

Those with TB ($n = 12$) demonstrated a SUVmax of 3.99 ± 2.28, a median value of 3.71 ($pct_{25} = 2.19$, $pct_{75} = 4.95$).In patients with other benign lesions ($n = 10$), the following values were observed: a SUVmax of 2.70 ± 1.31, a median value of 2.50 ($pct_{25} = 1.76$, $pct_{75} = 3.59$). The mean values of these three types of pathology were not statistically significant ($p = 0.1919$), and therefore the $SUVmax_1$ could not be used to accurately

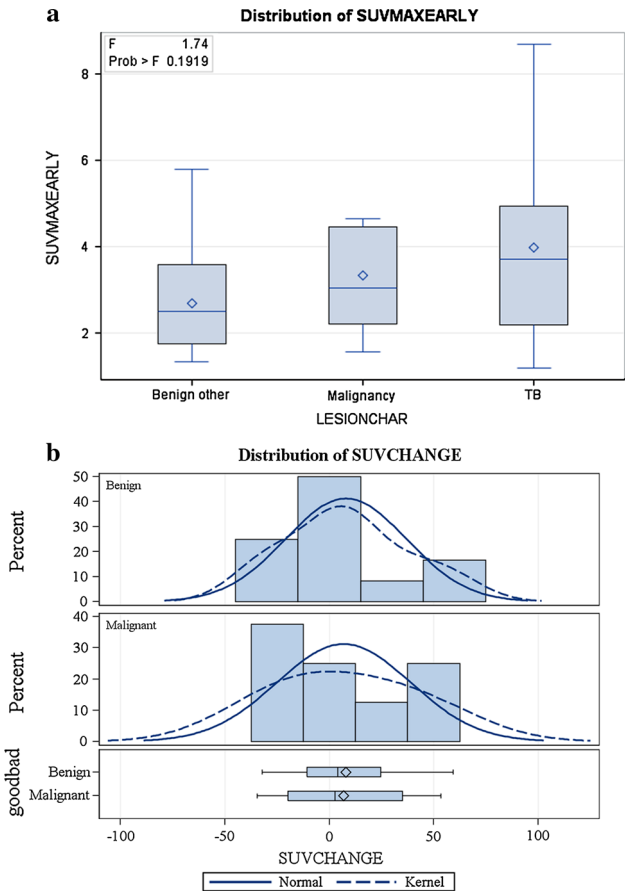

Fig. 2 **a** Boxplot demonstrating inability to distinguish between TB, malignant lesions and other benign lesions based on early SUVmax alone ($p = 0.19$). **b** Diagram representing the change between SUVmax early (60 min) and SUVmax delayed (120 min) and the inability to distinguish lesions based on a change in SUV. The distribution (histogram) of SUV change (percentage deviation between first and second measurement) is shown together with the normal (Gaussian) probability density function, calculated from mean and standard deviation (*solid line*), and the kernel density estimation (*dashed line*) which is a non-parametric way to estimate the probability density function of a random variable. When both curves are approximately equal, there is no evidence of non-normality. At the *bottom*, the boxplot is shown with mean (*diamond symbol*) and median (*vertical line* in the *box*)

distinguish between these lesions (Fig. 2a). Combining the last two groups mentioned into one benign group ($n = 22$) resulted in a mean SUVmax of 3.3 (±2, a minimum value of 1.19 and a maximum of 8.69). Again, no distinction could be made between benign ($n = 22$) and malignant ($n = 14$) lesions based on $SUVmax_1$ ($p = 0.9374$).

SUVmax at 120 min post-injection

Imaging at this time point also did not reveal any difference in the mean SUVmax between benign ($n = 11$) and malignant ($n = 9$) lung lesions ($p = 0.4024$).

Benign lesions demonstrated a mean SUVmax of 2.7 (1.65) compared to a mean SUVmax of 3.4 (1.9) in malignant lesions.

Dual-time point imaging (SUVmax at 60- and 120-min post-injection)

Benign lesions demonstrated a mean change between these values of 0.19 (0.15), ranging 0.02–0.49. Malignant lesions demonstrated a mean value of 0.29 (0.2), which ranged 0–0.59. These differences were not statistically significant ($p = 0.2299$) (Fig. 2b).

Differences in various lesions: background/reference ratios were also considered in order to distinguish benign from malignant lesions. These consisted of the SUVmax in the primary lesion relative to the SUVmax of the liver, spleen, bone marrow and mediastinal blood pool, none of which were statistically significant.

All of the malignant lesions (14/14) in this study (including two tumors of neuro-endocrine origin) demonstrated increased tracer accumulation (Fig. 3). In addition, malignant lung lesions (almost without exception) were associated with diffusely increased bone marrow uptake when compared to patients with benign lesions. However, this was not found to be statistically significant and may require a larger patient population for validation. Tuberculosis also demonstrated abnormal tracer accumulation (Fig. 4).

Five patients demonstrated no tracer accumulation in the lesions noted on CT and were found on histology not to have any malignant, infective or inflammatory changes (Fig. 5).

Finally, a comparison was made between PET and CT to determine which was more accurate at predicting the nature of a lesion. Making use of the above-described qualitative assessment or visual score, PET was considered correct, whenever these patterns were present. CT was considered correct whenever the final diagnosis was included in the diagnosis.

The following observations were made:

Using the above-mentioned expected patterns of uptake, ^{68}Ga-citrate PET (considered in isolation) performed as follows:

1. For benign lesions a 100 % sensitivity and a 100 % negative predictive value were calculated. Specificity and PPV were 57.7 and 47.6 %, respectively. For malignant lesions specificity was 77.3 %, NPV 77.3 %, sensitivity 64.3 % and PPV 64.3 %.
2. Distinguishing benign ($n = 22$) from malignant lesions ($n = 14$): sensitivity was 77.3 %, NPV 77.3 %, specificity 36 % and PPV 65.4 %. PET correctly predicted the nature of the lesion in 26/36 cases (72 %), compared to CT's correct prediction in 28/36 (77.78 %).

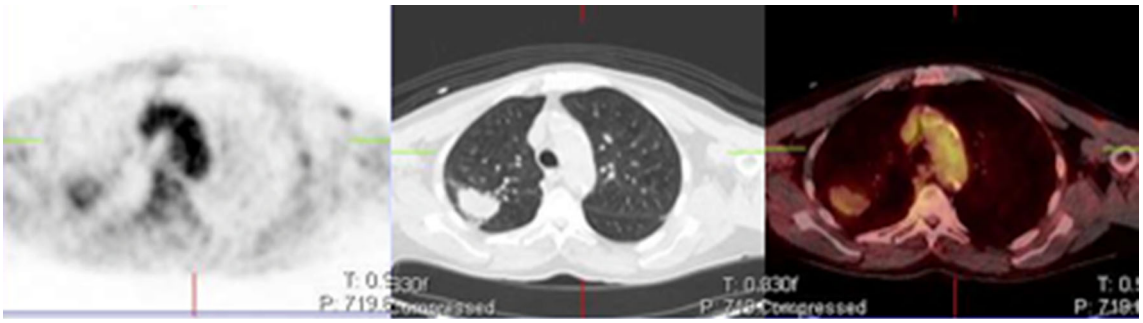

Fig. 3 A 74-year-old male smoker who presented with a *right upper* lobe mass on CXR. Transverse PET, CT and fused PET/CT images demonstrate increased tracer accumulation in the lung mass (SUVmax: 2.99). Histology revealed a moderately differentiated adenocarcinoma

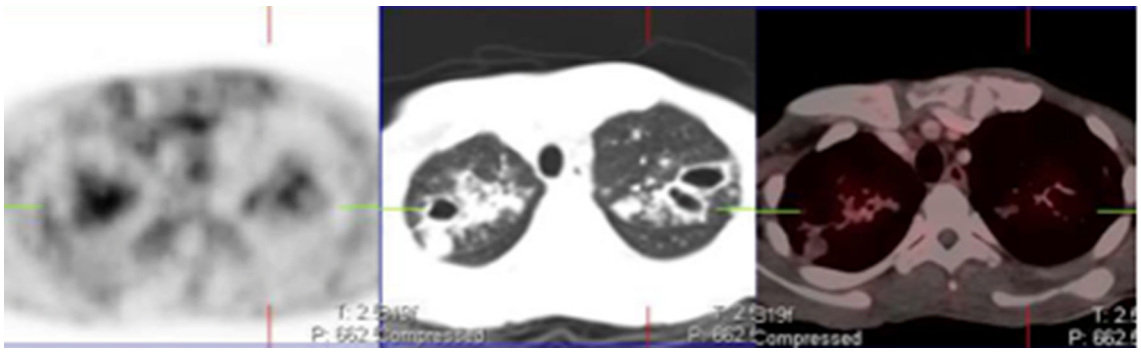

Fig. 4 A 44-year-old male smoker with RVD presented with bilateral apical lung changes. Transverse PET, CT and fused PET/CT images demonstrate increased tracer uptake in both apical lobes. Sputum cultures confirmed *Mycobacterium tuberculosis*

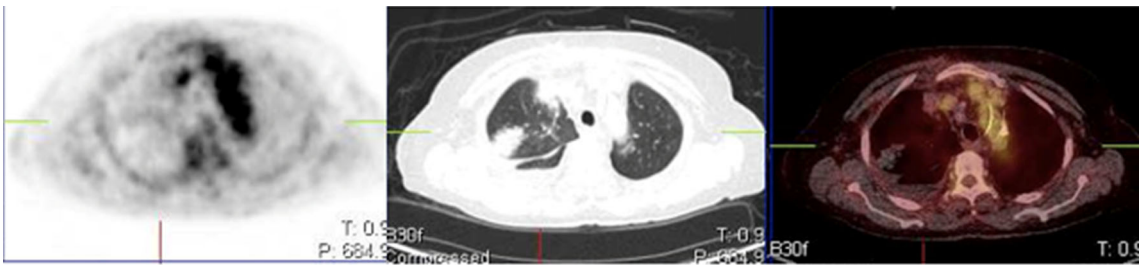

Fig. 5 A 71-year-old female smoker with a *right upper* lobe mass and pleural effusion. Transverse PET/CT images demonstrate no uptake in the afore-mentioned lesions. Histology did not reveal any malignant or inflammatory cells

Discussion

Distinguishing benign from malignant lesions in the lung continues to present a major problem, with no clear set of distinguishing features on conventional imaging to guide further patient management.

Although dual-phase imaging with ^{18}F-FDG has been shown to be useful in certain settings [19], it has not been helpful in settings with a high prevalence of granulomatous lung diseases. Often, a multitude of investigations are undertaken, which still often result in the need for bronchoscopy with biopsy for histological confirmation. Even then, histology may still not provide a clear answer.

There is renewed interest in ^{68}Ga-labeled compounds due to the many imaging advantages, which includes round-the-clock availability, the short half-life, labeling possibilities and anticipated higher cost-effectiveness, amongst many others.

Several authors have investigated the use of ^{68}Ga-citrate- and other ^{68}Ga-compounds [20–22] in the evaluation of various infectious and inflammatory conditions. So far, the most promising results have been found with the imaging of musculoskeletal infections [13, 14].

With this study we proposed the novel use of ^{68}Ga-citrate for imaging of lung lesions of an indeterminate nature. From our initial experience, the labeling method is

relatively simple, the image quality is good and dual-point imaging up to 2 h post-injection is possible. Also, the dosimetry compares favorably to that of ^{18}F-FDG [17] and normal bio-distribution does not include any lung uptake, which may provide good lesion to background ratios.

Our results demonstrated very low or absent tracer accumulation in lesions where no malignant or inflammatory cells could be demonstrated on histology. Other benign lesions, such as infective changes or sarcoidosis demonstrated slightly higher uptake, which was still relatively low to the uptake of malignant lesions. Malignant and tuberculous lesions, demonstrated higher ^{68}Ga-citrate uptake with considerable overlap in the SUVmax, which made accurate differentiation between these two processes impossible with this sample size.

The following observations or trends seem worth highlighting (despite the lack of statistical significance in this study):

1. All of the malignant lesions in this study (including two tumors of neuro-endocrine origin) demonstrated increased tracer accumulation, which may be indicative of few false negatives.
2. Malignant lung lesions were often associated with diffusely increased bone marrow uptake, which was more intense than that seen in patients with benign lesions. One possible explanation could be that malignant lesions are often accompanied by anemia of chronic disease, which may cause diffusely increased bone marrow and splenic uptake of ^{68}Ga-citrate. Another factor may be increased transferrin expression [23]. This could potentially bring about significant differences in ratios when using the RES as reference in trying to distinguish malignant from granulomatous lesions. This would require further investigation and validation in a larger sample.

Importantly, five patients in our study demonstrated no tracer accumulation in the lesions noted on CT and were found on histology not to have any malignant, infective or inflammatory changes. This indicates a possible role for ^{68}Ga-citrate as a tracer with a good negative predictive value. Patients who present with these photopenic lesions corresponding to suspicious lesions noted on morphological imaging, could therefore be followed up instead of having to undergo invasive diagnostic procedures, such as lung biopsy. All of the patients who had histology which did not reveal any malignant, inflammatory or infective cells, and demonstrated no uptake of ^{68}Ga-citrate in these lesions (100 % NPV).

The bio-distribution of ^{68}Ga-citrate demonstrated pronounced blood pool activity, which is different from the bio-distribution seen with ^{67}Ga-citrate and which has also been confirmed by other authors [14, 17]. Compared to ^{67}Ga-citrate, ^{68}Ga-citrate has a much shorter half-life (68 min vs. 78 h) and the ideal uptake time for imaging with ^{68}Ga-citrate has not yet clearly been established, due to (as yet) limited patient data. We found that good image quality was obtained at 60 and 120 min, with significant deterioration in quality after 150 min. It could be argued, however, that these early images reflect changes in tissue blood volume only and does not convey any information on transferrin receptor expression.

Considering the various uptake mechanisms that are involved in Gallium lesion accumulation, we postulated that the tracer kinetics may be different in malignant and infective kinetics and therefore empirically selected two time points: one at 60 min and one at 120 min.

Future considerations should include a large number of participants and compare the findings to ^{18}F-FDG. Furthermore improvements on the present study would be the addition of dynamic imaging with kinetic modeling and more imaging time points in order to evaluate different washout rates of ^{68}Ga-citrate in benign, malignant and tuberculous lesions. Quantification of lung lesions on PET could also be optimized.

Conclusion

This study, as the first human study using ^{68}Ga-citrate for in vivo lung pathology imaging, demonstrated that ^{68}Ga-citrate PET has a potential for detection of malignancy. Although it has higher ability to detect TB lesions than CT, ^{68}Ga-citrate seemed unable to provide a clear distinction between malignant and benign lung lesions in a setting with a high prevalence of granulomatous diseases such as TB. Larger trials are needed in order to better evaluate this novel application.

Acknowledgments The authors thank Thomas Ebenhan and Brenda Mokaleng for the labeling. The authors also thank the departments of nuclear medicine and radiology at Steve Biko Academic Hospital for imaging and interpretation and iThemba Labs for the generator.

Conflict of interest No conflicts of interest to declare.

References

1. Jones YM, Irion KL, Holemans JA. A review of the imaging and clinical management of solitary pulmonary nodules. Imaging. 2008;20:303–11.
2. Kim SK, Allen-Auerbach M, Goldin J, Fueger BJ, Dahlbom M, Brown M, et al. Accuracy of PET/CT in characterization of solitary pulmonary lesions. J Nucl Med. 2007;48:214–20.
3. Tsushima Y, Tateishi U, Uno H, Takeuchi M, Terauchi T, Goya T, et al. Diagnostic performance of PET/CT in differentiation of malignant and benign non-solid solitary pulmonary nodules. Ann Nucl Med. 2008;22:571–7.

4. Sathekge MM, Maes A, Kgomo M, Stoltz A, Pottel H, Van de Wiele C. Impact of FDG PET on the management of TBC treatment. A pilot study. Nuklearmedizin. 2009;49:35–40.
5. Sathekge MM, Maes A, Pottel H, Stoltz A, van de Wiele C. Dual time-point FDG PET-CT for differentiating benign from malignant solitary pulmonary nodules in a TB endemic area. S Afr Med J. 2010;100:598–601.
6. Alavi A, Gupta N, Alberini JL, Hickeson M, Adam LE, Bhargava P, et al. Positron emission tomography imaging in nonmalignant thoracic disorders. Semin Nucl Med. 2002;32:293–321.
7. Mavi A, Lakhani P, Zhuang H, Gupta NC, Alavi A. Fluorodeoxyglucose-PET in characterizing solitary pulmonary nodules, assessing pleural diseases, and the initial staging, restaging, therapy planning, and monitoring response of lung cancer. Radiol Clin North Am. 2005;43:1–21.
8. Tsan MF. Mechanism of gallium-67 accumulation in inflammatory lesions. J Nucl Med. 1985;26:88–92.
9. Weiner RE. The mechanism of ^{67}Ga localization in malignant disease. Nucl Med Biol. 1996;23:745–51.
10. Chen DC, Newman B, Turkall RM, Tsan MF. Transferrin receptors and gallium-67 uptake in vitro. Eur J Nucl Med. 1982;7:536–40.
11. Tsuchiya Y, Nakao A, Komatsu T, Yamamoto M, Shimokata K. Relationship between gallium 67 citrate scanning and transferrin receptor expression in lung diseases. Chest. 1992;102:530–4.
12. AL-Nahhas A, Win Z, Szyszko T, Singh A, Khan S, Rubello D. What can gallium-68 PET add to receptor and molecular imaging? Eur J Nucl Med Mol Imaging. 2007;34:1897–901.
13. Mäkinen TJ, Lankinen P, Pöyhönen T, Jalava J, Aro HT, Roivainen A. Comparison of 18F-FDG and ^{68}Ga PET imaging in the assessment of experimental osteomyelitis due to *Staphylococcus aureus*. Eur J Nucl Med Mol Imaging. 2005;32:1259–68.
14. Nanni C, Errani C, Boriani L, Fantini L, Ambrosini V, Boschi S, et al. ^{68}Ga-citrate PET/CT for evaluating patients with infections of the bone: preliminary results. J Nucl Med. 2010;51:1932–6.
15. de Blois E, Sze Chan H, Naidoo C, Prince D, Krenning EP, Breeman WAP. Characteristics of SnO_2-based ^{68}Ge/^{68}Ga generator and aspects of radiolabelling DOTA-peptides. Appl Radiat Isot. 2011;69:308–15.
16. Kumar V, Boddeti DK, Evans SG, Angelides S. $^{(68)}$Ga-citrate-PET for diagnostic imaging of infection in rats and for intra-abdominal infection in a patient. Curr Radiopharm. 2012;5:71–5.
17. Rizzello A, Di Pierro D, Lodi F, Trespidi S, Cicoria G, Pancaldi D, et al. Synthesis and quality control of ^{68}Ga citrate for routine clinical PET. Nucl Med Commun. 2009;30:542–5.
18. Miller RF. Nuclear medicine and AIDS. Eur J Nucl Med. 1990;16:103–18.
19. Lin YY, Chen JH, Ding HJ, Liang JA, Yeh JJ, Kao CH. Potential value of dual-time-point ^{18}F-FDG PET compared with initial single-time-point imaging in differentiating malignant from benign pulmonary nodules: a systematic review and meta-analysis. Nucl Med Commun. 2012;33:1011–8.
20. Kumar V, Boddeti DK, Evans SG, Roesch F, Howman-Giles R. Potential use of ^{68}Ga-apo-transferrin as a PET imaging agent for detecting *Staphylococcus aureus* infection. Nucl Med Biol. 2011;38:393–8.
21. Petrik M, Franssen GM, Haas H, Laverman P, Hörtnagl C, Schrettl M, et al. Preclinical evaluation of two $^{(68)}$Ga-siderophores as potential radiopharmaceuticals for *Aspergillus fumigatus* infection imaging. Eur J Nucl Med Mol Imaging. 2012;39:1175–83.
22. Ambrosini V, Zompatori M, De Luca F, Antonia D, Allegri V, Nanni C, et al. ^{68}Ga-DOTANOC PET/CT allows somatostatin receptor imaging in idiopathic pulmonary fibrosis: preliminary results. J Nucl Med. 2010;51:1950–5.
23. Wang SJ, Gao C, Chen BA. Advancement of the study on iron metabolism and regulation in tumor cells. Chin J Cancer. 2010;29:451–5.